

---

# Memory-Efficient Sparse Pyramid Attention Networks for Whole Slide Image Analysis

---

**Weiye Wu**

Dartmouth College  
Hanover, NH 03755  
weiyi.wu.gr@dartmouth.edu

**Chongyang Gao**

Northwestern University  
Evanston, IL 60208  
Chongyanggao2026@u.northwestern.edu

**Xinwen Xu**

Dartmouth College  
Hanover, NH 03755  
xinwen.xu.gr@dartmouth.edu

**Xingjian Diao**

Dartmouth College  
Hanover, NH 03755  
xingjian.diao.gr@dartmouth.edu

**Siting Li**

Dartmouth College  
Hanover, NH 03755  
siting.li.gr@dartmouth.edu

**Jiang Gui**

Dartmouth College  
Hanover, NH 03755  
jiang.gui@dartmouth.edu

## Abstract

Whole Slide Images (WSIs) are crucial for modern pathological diagnosis, yet their gigapixel-scale resolutions and sparse informative regions pose significant computational challenges. Traditional dense attention mechanisms, widely used in computer vision and natural language processing, are impractical for WSI analysis due to the substantial data scale and the redundant processing of uninformative areas. To address these challenges, we propose Memory-Efficient Sparse Pyramid Attention Networks with Shifted Windows (SPAN), drawing inspiration from state-of-the-art sparse attention techniques in other domains. SPAN introduces a sparse pyramid attention architecture that hierarchically focuses on informative regions within the WSI, aiming to reduce memory overhead while preserving critical features. Additionally, the incorporation of shifted windows enables the model to capture long-range contextual dependencies essential for accurate classification. We evaluated SPAN on multiple public WSI datasets, observing its competitive performance. Unlike existing methods that often struggle to model spatial and contextual information due to memory constraints, our approach enables the accurate modeling of these crucial features. Our study also highlights the importance of key design elements in attention mechanisms, such as the shifted-window scheme and the hierarchical structure, which contribute substantially to the effectiveness of SPAN in WSI analysis. The potential of SPAN for memory-efficient and effective analysis of WSI data is thus demonstrated, and the code will be made publicly available following the publication of this work.

## 1 Introduction

Whole Slide Images (WSIs) have become an indispensable tool in modern digital pathology, enabling the digitization of histopathological slides and facilitating computer-aided diagnosis [6, 1]. However, the gigapixel resolution of WSIs presents significant computational challenges for automated analysis, with the amount of data far surpassing the capacity of traditional image analysis techniques designed for natural images.

In recent years, deep learning has made remarkable progress across various domains, revolutionizing the way we approach and solve complex problems. This progress has been largely driven by the development of powerful architectures that can learn rich, hierarchical representations from vast amounts of data. In particular, the natural language processing (NLP) domain has witnessed significant breakthroughs with the introduction of transformer-based models [10, 5, 23]. These models have revolutionized tasks such as language understanding, generation, and translation by effectively capturing long-range dependencies and contextual information in text data. Similarly, the field of computer vision (CV) has experienced rapid advancements, primarily due to the success of convolutional neural networks (CNNs) [14, 25] and, more recently, Vision Transformers (ViTs) [12, 9, 11]. These state-of-the-art architectures have achieved exceptional performance in various tasks, including image classification, object detection, and semantic segmentation, by learning to extract meaningful features and representations from visual data.

While these advancements have revolutionized the field of deep learning and introduced attention mechanisms that effectively capture long-range dependencies and focus on relevant information [11, 24, 34, 10], they also present challenges in terms of scalability and efficiency. The quadratic complexity of dense attention presents a significant challenge when dealing with longer sequences or a larger number of data. Various techniques have been proposed to address this computational bottleneck. Sparse Transformers [40, 3] selectively attend to a subset of tokens, reducing computational complexity from quadratic to sub-quadratic. Linear Transformers [38, 17], on the other hand, approximate the self-attention mechanism to achieve linear computational complexity, enabling the processing of much longer sequences. Furthermore, there are many other advancements in general domains, such as position encoding techniques [32, 29]. The success of these advancements suggests the potential of applying similar techniques to the analysis of WSIs, as they may help address the challenges posed by the large, spatially complex nature of WSIs.

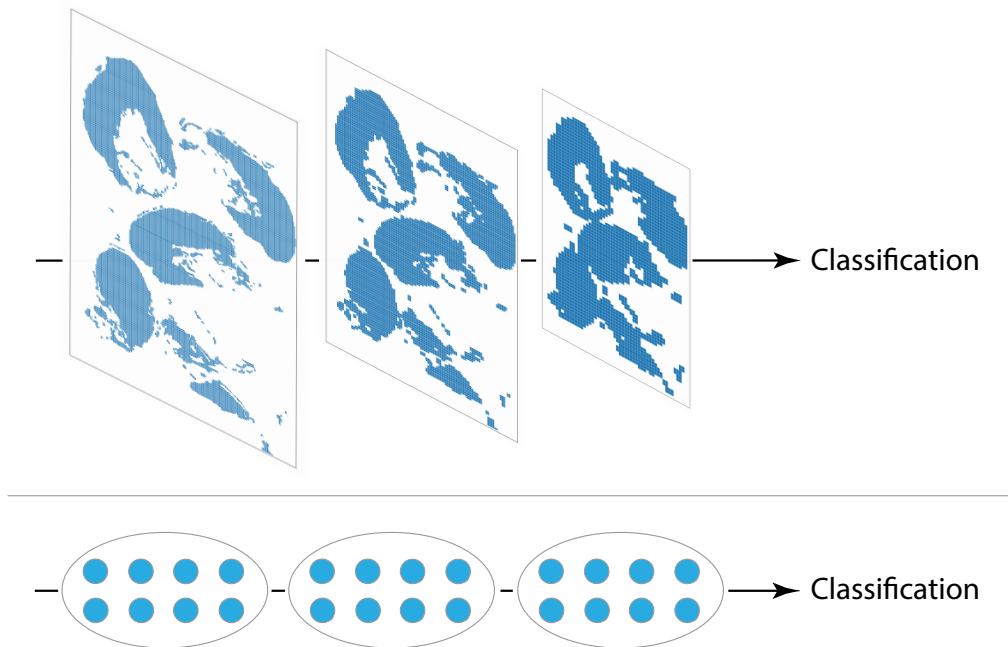


Figure 1: Comparison of our proposed hierarchical approach with conventional patch-based methods. Top: Our method constructs a hierarchical representation that captures spatial relationships and multi-scale contextual information. Bottom: Conventional methods treat patches as independent and identically distributed (i.i.d.) samples, ignoring the rich spatial structure present in the data.

The predominant paradigm in WSI analysis has been the adoption of a two-stage patch-based framework. This approach begins by segmenting WSIs into smaller, non-overlapping patches, with the background removed. Each patch is then processed by a fixed feature extractor to generate

high-dimensional feature representations. These features are aggregated using multiple instance learning (MIL) models, such as attention-based MIL (ABMIL) [16], to predict slide-level outcomes. While many WSI analysis methods focus on extending ABMIL by incorporating additional losses or training strategies [28, 19, 41, 30], they treat patches as independent and identically distributed (i.i.d.) entities (Figure 1, Bottom), overlooking the rich spatial structures and long-range dependencies intrinsic to WSIs. The gigapixel nature of WSIs and the presence of vast uninformative regions pose challenges to the direct application of the advancements in general CV and NLP for dependency modeling. To bridge this gap between general deep learning domains and WSI analysis, we propose Memory-Efficient Sparse Pyramid Attention Networks (SPAN). SPAN introduces a novel framework that efficiently leverages the hierarchical nature and long-range contextual information in WSIs while maintaining computational efficiency.

The key components of SPAN are designed to address the limitations of current patch-based methods. The sparse pyramid attention architecture hierarchically focuses on informative regions within the WSI, reducing computational overhead while preserving critical diagnostic features. By employing a pyramid structure, SPAN efficiently processes WSIs at multiple scales, capturing both local and global context. The sparse attention mechanism selectively attends to informative regions, alleviating the computational burden imposed by large, uninformative areas. Furthermore, SPAN incorporates shifted windows and global tokens to enhance the model’s ability to capture long-range contextual dependencies and global information. Moreover, SPAN is compatible with various general-purpose techniques, allowing for seamless integration and adaptation to the specific properties of WSI data. This flexibility opens up opportunities for future exploration and refinement of the SPAN framework.

The main contributions of this paper are as follows:

- We propose SPAN, a novel framework that combines sparse pyramid attention with shifted windows, specifically designed for efficient and effective WSI analysis.
- We introduce a sparse pyramid attention architecture that hierarchically focuses on informative regions, reducing computational complexity while preserving critical diagnostic features.
- We incorporate shifted windows and global information carrier tokens to enhance the model’s ability to capture long-range contextual dependencies, which are essential for accurate disease classification.
- We evaluate SPAN on multiple public WSI datasets, demonstrating its superior performance compared to state-of-the-art methods in downstream classification tasks. Our approach enables the precise modeling of both spatial and contextual information, which is often challenging for existing methods due to memory constraints.

## 2 Related Works

### 2.1 Attention Mechanisms

Attention mechanisms, particularly self-attention, have revolutionized various domains, including natural language processing (NLP) and computer vision (CV). The introduction of Transformer-based models, such as BERT [10] and GPT [5], has marked a paradigm shift from traditional recurrent neural networks in language modeling. By leveraging the power of self-attention to capture long-range dependencies in text, Transformers have achieved state-of-the-art performance on a wide range of tasks, establishing themselves as the dominant architecture in NLP. However, the quadratic computational complexity of self-attention can be prohibitive for processing long sequences. To address this issue, sparse attention mechanisms, such as Longformer [3] and BigBird [40], have been proposed, limiting the attention computation to fixed windows and significantly reducing the computational complexity while still capturing important long-range dependencies.

The Vision Transformer (ViT) [11] has challenged the long-standing dominance of convolutional neural networks (CNNs) by demonstrating the effectiveness of self-attention in learning visual representations. To further improve the performance and efficiency of ViT, several variants, such as Swin Transformer [24] and FasterViT [12], introduce window attention mechanisms. Unlike in NLP, where window attention is primarily used to reduce computational complexity, the main purpose of window attention in CV is to introduce a hierarchical structure and incorporate inductive biases, leading to state-of-the-art performance on various computer vision tasks.

Position encoding is another crucial aspect of attention mechanisms, allowing the model to incorporate positional information of the input tokens. In NLP, absolute position encoding [34, 10, 22] and relative position encoding [31, 8] have been widely studied. Similarly, research on position encoding in ViT has been a highly active area, ranging from the initial Absolute Position Embedding (APE) [11] to the more recent Relative Position Bias (RPB) [24]. Recent studies have also actively sought to introduce rotary position encoding techniques from large language models (LLMs) into CV models to enhance the performance of downstream classification, segmentation tasks, and high-resolution image generation [27, 12, 15]. The combined use of self-attention mechanisms and position encoding has substantially improved models' ability to capture long-range dependencies and relationships, enhancing their performance across a wide range of tasks.

## 2.2 Pyramid Structures in Computer Vision

The concept of multi-scale feature extraction and representation has been a fundamental aspect of computer vision for decades. Unlike in natural language processing, where data is often treated uniformly, visual data is inherently hierarchical, with information present at various scales. The early recognition of this hierarchical nature can be traced back to seminal works like SIFT descriptors [26], which employed a scale-space pyramid to extract scale-invariant features.

The advent of deep learning and CNNs further ingrained the importance of hierarchical processing in computer vision. From the pioneering AlexNet [18] to more advanced architectures like ResNet [14] and ConvNeXt [25], CNNs inherently process visual data in a hierarchical manner. The progressive downsampling of feature maps and increase in channel depth allow these networks to capture features at multiple scales, with shallow layers extracting fine details and deeper layers capturing more abstract semantics. Building upon this implicit hierarchical structure, we propose explicit pyramid architectures to further enhance the multi-scale capabilities of CNNs. SPP-Net [13] introduced spatial pyramid pooling to aggregate context at multiple scales, inspiring a wave of multi-scale CNN designs. FPN [20] proposed a top-down architecture with lateral connections to build high-level semantic feature maps at all scales. HRNet [35] took a different approach, maintaining high-resolution representations throughout the network via parallel multi-resolution convolutions and repeated multi-scale fusions.

The crucial role of pyramid structures has been recognized in ViTs as well. While the original ViT [11] processes image patches uniformly using an isotropic structure, many subsequent studies have explored integrating pyramid structures with efficient attention mechanisms to enhance the performance and efficiency of ViTs. The PVT [37] integrates pyramid structures into the transformer architecture, progressively reducing spatial resolution and increasing channel dimension to create a hierarchical representation. The Swin Transformer [24] combines a hierarchical design with a shifted window mechanism to enable better cross-window information exchange. The Focal Transformer [39] proposes a focal self-attention mechanism that operates on both fine-grain and coarse-grain levels, creating a multi-level hierarchy. FasterViT [12] combines CNNs and ViTs with carrier tokens to facilitate global information exchange among local windows at different scales. These concurrent developments reinforce the fundamental importance of multi-scale pyramid representation learning in computer vision.

## 2.3 Whole Slide Image Analysis: Characteristics and Challenges

The advancements in transformer-based models, as well as the effectiveness of pyramid structures in capturing multi-scale information, have the potential to improve performance significantly in the NLP and CV domains. However, applying these advancements directly to WSIs is challenging due to their sparse nature post-preprocessing and their gigapixel size.

The original WSIs are typically stored in a pyramid format, with multiple magnification levels available for pathologists to examine the tissue at different scales. However, the pyramid structure underscores the importance of hierarchical information for human analysis of WSIs.

However, mainstream WSI analysis methods typically operate in an isotropic fashion, treating input data uniformly without considering the inherent multi-scale nature of the WSI pyramid structure [28, 16, 19, 41, 33]. These methods are built upon ABMIL [16]. For instance, CLAM [28] utilizes an additional network to predict patches with high attention scores from ABMIL, grouping them into the same class as the corresponding WSIs. MHIM [33] employs a Siamese ABMIL network's attention

outputs to drop patches randomly. DTFD [41] divides bags into sub-bags and uses these sub-bags for ABMIL training. However, these approaches fail to capture the crucial spatial and hierarchical features necessary for accurate WSI analysis. Another approach, introduced by TransMIL [30], flattens patches into a sequence and then reshapes them into a square to preserve some spatial information. Nonetheless, this method distorts the true spatial relationships and may not perform well in certain situations, also ignoring hierarchical information.

Drawing from the success of multi-scale and hierarchical structures in computer vision and the advancements in position encoding techniques, it is evident that effectively incorporating spatial information and multi-scale features in WSI analysis is crucial. Our proposed framework, SPAN, employs an efficient encoding strategy that enables precise analysis of WSIs with feasible memory usage and speed, making it possible to use the same modeling techniques as in other active research domains.

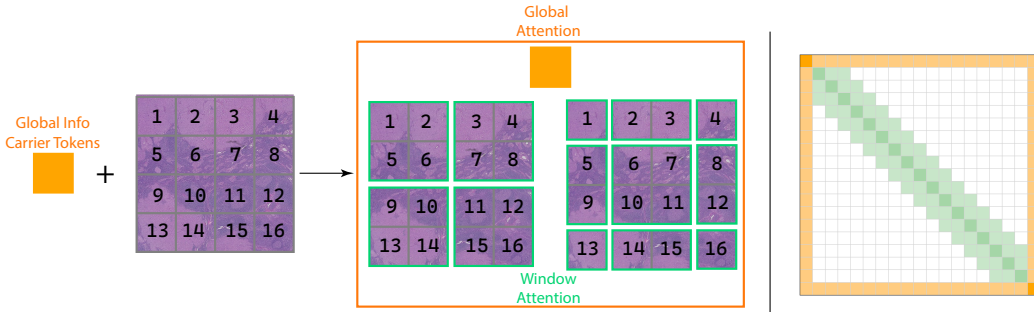


Figure 2: Schematic of the proposed sparse window attention mechanism. The input WSI is partitioned into non-overlapping  $2w \times 2w$  windows using an index-driven approach that leverages the inherent sparsity of WSIs. The windows are then shifted by  $w \times w$  to obtain a second set of non-overlapping windows. Local attention is computed within each window (green boxes), while global attention is captured via learnable global tokens (orange box) that interact with all tokens in the WSI. This architecture efficiently captures both local details and long-range dependencies while minimizing memory overhead. The right figure visualizes the pattern of interactions between local and global tokens.

### 3 Method

#### 3.1 Overview

SPAN is a sparse pyramid attention architecture designed for efficient and effective WSI analysis. The main components of SPAN include a sparse convolutional block, a window generation block, and a sparse attention block. Given the inputs, a feature matrix, and a coordinates matrix, SPAN first indexes the inputs. The architecture alternates between parameterized convolutional layers and parameterized sparse attention layers. The sparse attention layers capture local dependencies within the windows, as well as long-range dependencies with global attention. This process focuses on informative regions and interactions at the current scale. The convolutional layers gradually reduce the spatial resolution to capture spatial and hierarchical features. The pipeline of the SPAN architecture is presented in Figure 3. Finally, the classification head aggregates the learned features to make a slide-level prediction.

#### 3.2 Window Generation Block

Given feature inputs  $\mathbf{X} \in \mathbb{R}^{N \times d}$ , where  $N$  is the number of non-empty patches and  $d$  is the feature dimension, conventional window generation methods [24, 3, 40] used in general domains are likely suboptimal in terms of efficiency for our sparse matrix scenario. These methods typically operate directly on dense feature matrices, obtaining different views of the same dense matrix by striding over a certain number of elements in the matrix’s memory. However, due to the sparsity of the matrix positions, applying the same processing method would require first padding the feature matrix and coordinate matrix into a dense form. Since  $d$  is usually large, this approach would lead to a

significant increase in memory consumption and computational overhead due to the inclusion of many unnecessary padding operations.

To address this issue in window generation, we propose a block that utilizes indices for efficient window generation and attention mechanisms. By performing padding on the index matrix and using indices to specify the subsequent window attention computation, we avoid the padding of high-dimensional zero vectors and the duplication of feature matrices. The process, as illustrated in Figure 2, is a parallelizable high-speed module that involves only index operations and execution.

We represent the input WSI as a sparse tensor  $\mathbf{X} \in \mathbb{R}^{N \times d}$ , and coordinates inputs  $\mathbf{C} \in \mathbb{N}^{N \times 2}$ . Additionally, we introduce an index matrix  $\mathbf{I} \in \mathbb{N}^{N \times 1}$  that encodes the original spatial locations of the non-empty patches, establishing an index-feature-position mapping. This mapping allows us to perform padding operations on the 1D index matrix instead of directly padding the high-dimensional feature vectors, thereby substantially reducing memory overhead. The window generation block proceeds as follows:

---

**Algorithm 1** Window Generation Block

---

**Require:** Patch features  $\mathbf{X} \in \mathbb{R}^{N \times d}$ , patch coordinates  $\mathbf{C} \in \mathbb{N}^{N \times 2}$ , window size  $w$

- 1:  $\mathbf{I} \leftarrow \text{range}(1, N + 1)$  ▷ Generate index vector
- 2:  $\mathbf{S} \leftarrow \text{sparse\_to\_dense}(\mathbf{C}, \mathbf{I})$  ▷ Convert sparse vectors to dense matrix
- 3:  $\mathbf{D} \leftarrow \text{generate\_windows}(\mathbf{S}, 2w)$  ▷ Generate non-overlapping windows of size  $2w \times 2w$
- 4:  $\mathbf{P} \leftarrow \text{pad\_zeros}(\mathbf{S}, w)$  ▷ Pad dense matrix with  $w$  on all sides
- 5:  $\mathbf{D}' \leftarrow \text{generate\_windows}(\mathbf{P}, 2w, w)$  ▷ Generate shifted windows of size  $2w \times 2w$  with stride  $w$
- 6:  $\mathbf{W} \leftarrow \text{filter\_zeros}(\mathbf{D} \cup \mathbf{D}')$  ▷ Filter out zeros within windows
- 7:  $\mathbf{G} \leftarrow \text{gather}(\mathbf{X}, \mathbf{W})$  ▷ Gather corresponding window features
- 8: **return**  $\mathbf{G}$

---

### 3.3 Parameterized Feature Extraction Block

Our proposed model incorporates parameterized feature extraction blocks that enable the efficient capture of hierarchical features and long-range dependencies in sparse WSIs. The architecture is composed of two kinds of layers: convolutional layers and transformer layers.

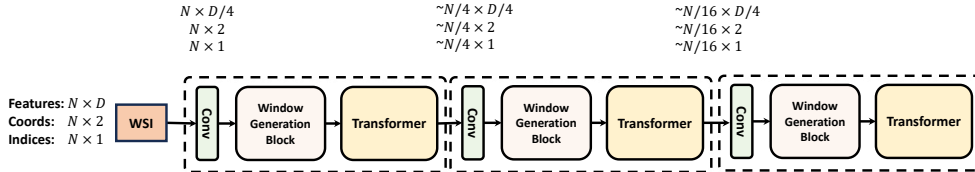


Figure 3: The figure illustrates the overall architecture of the SPAN model. The input WSI first passes through a  $1 \times 1$  convolution block for initial feature transformation, yielding patch-level features of size  $D/4$ . The Window Generation block then constructs local window features along with their coordinates and indices, which are fed into the Transformer block for attention computation and context modeling. Subsequently, the convolution block downsamples the feature map by a factor of approximately 4. The downsampling process is repeated hierarchically two times, with a convolution module performing sparse downsampling before each Transformer block, thereby preventing rapid memory consumption growth.

**Convolutional Layers** Given the sparse nature of the input features  $\mathbf{X} \in \mathbb{R}^{N \times d}$  and their corresponding positions  $\mathbf{C} \in \mathbb{R}^{N \times 2}$ , we employ sparse convolutions [7, 21] to perform downsampling and feature encoding. Sparse convolutions operate directly on the non-zero elements of the input, making them computationally efficient and memory-friendly compared to dense convolutions.

In the first feature extraction block, we apply a  $1 \times 1$  convolution to the input features to avoid direct downsampling and preserve the initial spatial resolution. This helps to maintain the fine-grained details of the input data. In subsequent layers, sparse convolutions with a kernel size of 2 and a

stride of 2 are used to downsample the spatial shape progressively. This downsampling operation reduces the number of patches by approximately a factor of 4, resulting in a hierarchical encoding structure. The reduction in the number of patches also accelerates subsequent attention computations and improves both computational and memory efficiency.

**Transformer Layers** After the convolutional layers, we leverage the sparse window attention mechanism by utilizing the computation graph generated by the window generation block. It involves customized graph operations to efficiently manage sparse data structures and optimize the attention mechanism [36]. This block generates both non-overlapping and shifted windows, and the Transformer layers utilize these windows to perform attention computations within local contexts. By using indices computed from these non-overlapping and shifted windows, we avoid duplicating a large number of samples and can perform transformer operations directly on the original feature vectors.

Although this approach extends the receptive field and captures dependencies within shifted windows, it may still fall short in capturing long-range dependencies beyond windows. To address this limitation, we introduce learnable global information carrier tokens. These tokens serve as a global context that can be accessed by all patch tokens, regardless of their local window. By attending to the global tokens, each patch token can incorporate global information into its representation. Similarly, the global tokens attend to all patch tokens, allowing them to gather information from the entire input sequence. This bidirectional interaction between global tokens and patch tokens enables the model to capture long-range dependencies that span multiple windows, enhancing its ability to model complex relationships within the WSI.

We initialize learnable relative position biases of size  $(2w + 1) \times (2w + 1)$  to encode positional information within each window, enhancing the model’s ability to consider the relative spatial arrangement of tokens. In all models, the window size  $w$  is set to a default value of 6.

### 3.4 Classification Head

After stacking three blocks, we obtain a condensed and hierarchical representation of the WSI. To perform the final classification task, we introduce an additional attention pooling layer to aggregate the obtained feature maps for classification.

Unlike traditional CNNs that often employ global average pooling or max pooling for final feature aggregation, we use an attention pooling layer. This choice is driven by the unique characteristics of WSI data. Even after two downsampling steps, the number of samples (i.e., patches) remains relatively large and varies considerably between different WSIs. Simple pooling methods may not be effective in handling this variability and could lead to a loss of important information. The attention pooling layer dynamically weights the importance of each patch based on its contribution to the final classification task.

## 4 Experiments

### 4.1 Experimental Setup

To evaluate the performance of our proposed SPAN architecture, we conducted experiments on two open WSI datasets: CAMELYON-16 [2] and BRACS [4]. We adhered to the official training, validation, and test splits provided by the datasets. If an official split was not available, we used the following protocol:

- **Test Set Splitting:** If the official test set is not provided, we randomly selected one-third of the samples as the test set with seed 42.
- **Validation Set Splitting:** If the official validation set is not provided, we randomly selected 15% of the training set as the validation set with seed 42.

The preprocessing pipeline adopted in this study is almost identical to that of CLAM [28] for all the datasets, with an additional crucial step introduced to align the patches with a grid of patch-sized cells. This alignment step is essential for preserving the spatial relationships between patches accurately. By extending the patch boundaries to the nearest multiple of the patch size (e.g., 224), we ensure that the

Table 1: Comparison of methods on the CAMELYON-16 dataset with statistical significance (p-values) compared to SPAN.

Method	CAMELYON-16					
	Accuracy	AUC	p-value	Runtime	Parameter Size	Memory Use
<b>ABMIL backbone</b>						
ABMIL	$0.867 \pm 0.023$	$0.880 \pm 0.031$	0.08	3.09s	0.59M	1.94GB
CLAM-SB	$0.881 \pm 0.014$	$0.875 \pm 0.017$	0.26	3.29s	0.79M	2.21GB
CLAM-MB	$0.870 \pm 0.033$	$0.884 \pm 0.030$	0.22	3.36s	0.79M	2.21GB
DFTD	$0.843 \pm 0.030$	$0.892 \pm 0.013$	0.02	3.25s	0.79M	1.77GB
MHIM	$0.876 \pm 0.015$	$0.871 \pm 0.027$	0.13	7.02s	0.59M	1.96GB
<b>TransMIL backbone</b>						
TransMIL	$0.805 \pm 0.115$	$0.819 \pm 0.152$	0.01	16.96s	2.67M	15.89GB
<b>SPAN backbone</b>						
SPAN	$0.893 \pm 0.017$	$0.908 \pm 0.024$	-	13.48s	2.37M	3.24GB

*Note:* Memory use is the GPU memory usage peak during training. Runtime is measured as the average time taken to complete one epoch of training and validation under the same condition. MHIM’s runtime includes the initialization step, so it is approximately doubled.

Table 2: Comparison of methods on the BRACS dataset with statistical significance (p-values) comparing with SPAN.

Method	BRACS				
	Accuracy	AUC (Negative)	AUC (Atypical)	AUC (Positive)	p-value
<b>ABMIL backbone</b>					
ABMIL	$0.639 \pm 0.015$	$0.823 \pm 0.023$	$0.647 \pm 0.017$	$0.900 \pm 0.018$	0.01
CLAM-SB	$0.616 \pm 0.026$	$0.778 \pm 0.013$	$0.638 \pm 0.027$	$0.894 \pm 0.010$	0.00
CLAM-MB	$0.623 \pm 0.027$	$0.804 \pm 0.014$	$0.676 \pm 0.011$	$0.902 \pm 0.016$	0.00
DFTD	$0.614 \pm 0.039$	$0.827 \pm 0.022$	$0.645 \pm 0.020$	$0.891 \pm 0.014$	0.00
MHIM	$0.634 \pm 0.021$	$0.801 \pm 0.021$	$0.636 \pm 0.025$	$0.910 \pm 0.036$	0.00
<b>TransMIL backbone</b>					
TransMIL	$0.602 \pm 0.024$	$0.796 \pm 0.037$	$0.665 \pm 0.027$	$0.868 \pm 0.016$	0.00
<b>SPAN backbone</b>					
SPAN	$0.690 \pm 0.028$	$0.870 \pm 0.030$	$0.692 \pm 0.059$	$0.900 \pm 0.019$	-

patch dimensions are consistent with the input grid of the model. This approach allows the patches to be seamlessly mapped to integer coordinates, maintaining the true spatial relationships between patches. In contrast, the patch coordinates would be floating-point values without this alignment step, requiring rounding to the nearest integers. This rounding process can potentially distort the spatial relationships between patches. This preprocessing step may result in a slightly larger number of patches compared to the original CLAM preprocessing pipeline. In line with common practice in WSI analysis, we employed a ResNet50 encoder as the feature extractor in our experiments. Specifically, we used the outputs of the penultimate layer of the ResNet50 encoder.

To ensure reproducibility and consistency across experiments, we used fixed random seeds. Each baseline model was run five times with different random initializations to account for variability in training. All the models adhered to the same hyperparameter settings, with a learning rate of  $1e-4$ , the AdamW optimizer, and a weight decay of  $5e-5$ .

## 4.2 Main Results

Table 1 and Table 2 demonstrate that our proposed SPAN method significantly outperforms existing baselines on the CAMELYON-16 and BRACS datasets in terms of accuracy and AUC. It’s worth noting that TransMIL shows significant instability on the CAMELYON-16, with one run completely failing to learn any effective features, leading to much worse performance. Although SPAN incurs



Table 3: Ablation study results for different model configurations, comparing the impact of position encoding, aggregation methods, global token presence, pyramid structure, and shifted-window mechanisms on model performance.

Configuration	Accuracy	AUC
<b>Aggregation</b>		
Global Token	$0.885 \pm 0.010$	$0.887 \pm 0.026$
<b>Positional Encoding</b>		
Axial Alibi	$0.888 \pm 0.014$	$0.903 \pm 0.016$
Axial RoPE	$0.878 \pm 0.013$	$0.855 \pm 0.019$
None	$0.885 \pm 0.008$	$0.899 \pm 0.013$
<b>Global Token Presence</b>		
No Global Token	$0.874 \pm 0.008$	$0.898 \pm 0.019$
<b>Pyramid Structure</b>		
No Downsampling	$0.879 \pm 0.024$	$0.879 \pm 0.014$
<b>Shifted Window</b>		
No Shifted Window	$0.878 \pm 0.008$	$0.894 \pm 0.007$
Baseline	$0.893 \pm 0.017$	$0.908 \pm 0.024$

higher computational costs, we argue that the substantial performance gains justify this, considering the importance of accuracy in medical diagnosis. The results suggest that SPAN’s architecture, designed to capture hierarchical structure and long-range dependencies in WSIs, contributes to its performance, highlighting its potential for enhancing the accuracy of computational pathology workflows.

### 4.3 Ablation Studies

To assess the contributions of various components of our model to its performance, we conducted ablation studies using the CAMELYON-16 dataset. The baseline model includes learnable relative position biases, attention pooling layers, a global token, a pyramid structure with downsampling convolutional layers, a window size of 6, and a shifted-window mechanism. We modified aspects such as position encoding, aggregation methods, the presence or absence of global is, pyramid structure, shifted-window mechanisms, and window sizes to explore different configurations and their effects on model performance.

The ablation study results (Table 3) demonstrate the robustness and flexibility of our model. Even without positional encoding, our model performs well, probably due to the inherent positional information captured by the shifted-window attention and convolutional layers. Moreover, our model is compatible with various advanced positional encodings from other domains, such as Alibi and RoPE, highlighting its extensibility to integrate future advancements in positional encoding techniques. Although these advanced encodings do not currently outperform our baseline with learnable relative position biases, future work may uncover more suitable frequencies or variants tailored to WSI characteristics, further enhancing model performance. Crucially, our experiments underscore the importance of the shifted-window mechanism and hierarchical downsampling through convolutional layers in WSI analysis. Unlike textual data with a 1D sequential structure, WSIs possess a 2D spatial structure. This necessitates careful consideration of adjacent regions. The shifted window mechanism ensures effective communication between adjacent windows, capturing essential spatial relationships. Without this mechanism, as demonstrated by the performance drop in the ablation study, non-overlapping windows would result in some adjacent visual tokens failing to compute any attention interactions. Additionally, the removal of the pyramid structure, i.e., downsampling convolutional layers, led to a decrease in performance, highlighting its importance in capturing multi-scale features. Furthermore, we observed that increasing the window size beyond a certain point does not necessarily improve performance. This is despite the higher computational resources used (Figure 4). This phenomenon may be attributable to diminishing returns on capturing long-range dependencies and increased complexity in the learning process, which can hinder the model’s efficiency at generalizing from training data as the window size becomes excessively large.

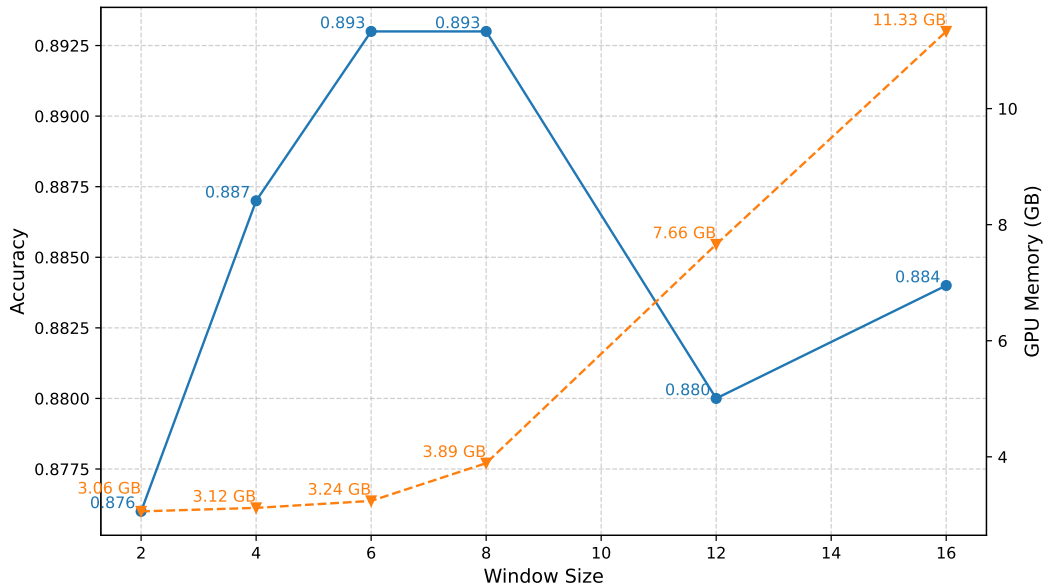


Figure 4: Accuracy and memory usage of SPAN with varying window sizes from  $2 \times 2$  to  $16 \times 16$ . Each configuration is evaluated over 5 runs, with the mean accuracy and peak memory usage reported. The results indicate that increasing the window size beyond a certain point does not necessarily improve performance but considerably increases memory usage.

We recommend that future research in WSI analysis consider incorporating these techniques to improve performance and carefully balance window size and computational efficiency. Lastly, our experiments with global tokens show that they are effective in carrying global information. Although using the global token representation directly for classification did not outperform the additional attention pooling layer, it still yielded competitive results. This finding suggests that global tokens can be a valuable tool for capturing global context in WSI analysis.

## 5 Conclusion and Limitations

We introduced SPAN, a memory-efficient Sparse Pyramid Attention Network designed specifically for the analysis of gigapixel Whole Slide Images (WSIs). In our experiments, SPAN demonstrated competitive performance in downstream WSI classification tasks. However, we recognize several limitations of our approach. Despite SPAN’s compatibility with a variety of positional encoding techniques, directly applying modern encoding methods did not yield performance improvements in our tests. Future research could explore learnable positional encoding frequencies or WSI-specific frequency values to potentially further enhance SPAN’s effectiveness. Our ablation studies also highlight the critical roles of the downsampling pyramid structure and the shifted-window mechanism in the efficacy of sparse attention models for WSI analysis. These elements are crucial to SPAN’s performance and could inform future innovations in this field.

In conclusion, SPAN represents a notable development in the efficient analysis of gigapixel WSIs, offering enhanced accuracy and reduced computational demands in our studies. Opportunities for further enhancements remain, such as extending SPAN’s applications to additional tasks like segmentation and integrating insights from related fields. Addressing these challenges could lead to more accurate, reliable, and efficient tools for computer-aided diagnosis in pathology.

## References

- [1] Esther Abels, Liron Pantanowitz, Famke Aeffner, Mark D Zarella, Jeroen van der Laak, Marilyn M Bui, Venkata NP Vemuri, Anil V Parwani, Jeff Gibbs, Emmanuel Agosto-Arroyo, et al. Computational pathology definitions, best practices, and recommendations for regulatory guidance: a white paper from the digital pathology association. *The Journal of pathology*, 249(3):286–294, 2019.
- [2] Babak Ehteshami Bejnordi, Mitko Veta, Paul Johannes Van Diest, Bram Van Ginneken, Nico Karssemeijer, Geert Litjens, Jeroen AWM Van Der Laak, Meyke Hermsen, Quirine F Manson, Maschenka Balkenhol, et al. Diagnostic assessment of deep learning algorithms for detection of lymph node metastases in women with breast cancer. *Jama*, 318(22):2199–2210, 2017.
- [3] Iz Beltagy, Matthew E Peters, and Arman Cohan. Longformer: The long-document transformer. *arXiv preprint arXiv:2004.05150*, 2020.
- [4] Nadia Brancati, Anna Maria Anniciello, Pushpak Pati, Daniel Riccio, Giosuè Scognamiglio, Guillaume Jaume, Giuseppe De Pietro, Maurizio Di Bonito, Antonio Foncubierta, Gerardo Botti, et al. Bracs: A dataset for breast carcinoma subtyping in h&e histology images. *Database*, 2022:baac093, 2022.
- [5] Tom Brown, Benjamin Mann, Nick Ryder, Melanie Subbiah, Jared D Kaplan, Prafulla Dhariwal, Arvind Neelakantan, Pranav Shyam, Girish Sastry, Amanda Askell, et al. Language models are few-shot learners. *Advances in neural information processing systems*, 33:1877–1901, 2020.
- [6] Gabriele Campanella, Matthew G Hanna, Luke Geneslaw, Allen Miraflor, Vitor Werneck Krauss Silva, Klaus J Busam, Edi Brogi, Victor E Reuter, David S Klimstra, and Thomas J Fuchs. Clinical-grade computational pathology using weakly supervised deep learning on whole slide images. *Nature medicine*, 25(8):1301–1309, 2019.
- [7] Spconv Contributors. Spconv: Spatially sparse convolution library. <https://github.com/traveller59/spconv>, 2022.
- [8] Zihang Dai, Zhilin Yang, Yiming Yang, Jaime Carbonell, Quoc Le, and Ruslan Salakhutdinov. Transformer-XL: Attentive language models beyond a fixed-length context. In *Proceedings of the 57th Annual Meeting of the Association for Computational Linguistics*, pages 2978–2988. Association for Computational Linguistics, 2019. doi: 10.18653/v1/P19-1285. URL <https://aclanthology.org/P19-1285>.
- [9] Timothée Darcet, Maxime Oquab, Julien Mairal, and Piotr Bojanowski. Vision transformers need registers. In *The Twelfth International Conference on Learning Representations*, 2024. URL <https://openreview.net/forum?id=2dn03LLiJ1>.
- [10] Jacob Devlin, Ming-Wei Chang, Kenton Lee, and Kristina Toutanova. Bert: Pre-training of deep bidirectional transformers for language understanding. *arXiv preprint arXiv:1810.04805*, 2018.
- [11] Alexey Dosovitskiy, Lucas Beyer, Alexander Kolesnikov, Dirk Weissenborn, Xiaohua Zhai, Thomas Unterthiner, Mostafa Dehghani, Matthias Minderer, Georg Heigold, Sylvain Gelly, Jakob Uszkoreit, and Neil Houlsby. An image is worth 16x16 words: Transformers for image recognition at scale. In *International Conference on Learning Representations*, 2021. URL <https://openreview.net/forum?id=YicbFdNTTy>.
- [12] Ali Hatamizadeh, Greg Heinrich, Hongxu Yin, Andrew Tao, Jose M. Alvarez, Jan Kautz, and Pavlo Molchanov. Fastervit: Fast vision transformers with hierarchical attention. In *The Twelfth International Conference on Learning Representations*, 2024. URL <https://openreview.net/forum?id=kB4yBiNmXX>.
- [13] Kaiming He, Xiangyu Zhang, Shaoqing Ren, and Jian Sun. Spatial pyramid pooling in deep convolutional networks for visual recognition. *IEEE transactions on pattern analysis and machine intelligence*, 37(9):1904–1916, 2015.

- [14] Kaiming He, Xiangyu Zhang, Shaoqing Ren, and Jian Sun. Deep residual learning for image recognition. In *Proceedings of the IEEE conference on computer vision and pattern recognition*, pages 770–778, 2016.
- [15] Byeongho Heo, Song Park, Dongyoon Han, and Sangdoon Yun. Rotary position embedding for vision transformer. *arXiv preprint arXiv:2403.13298*, 2024.
- [16] Maximilian Ilse, Jakub Tomczak, and Max Welling. Attention-based deep multiple instance learning. In *International conference on machine learning*, pages 2127–2136. PMLR, 2018.
- [17] Angelos Katharopoulos, Apoorv Vyas, Nikolaos Pappas, and François Fleuret. Transformers are rnns: Fast autoregressive transformers with linear attention. In *International conference on machine learning*, pages 5156–5165. PMLR, 2020.
- [18] Alex Krizhevsky, Ilya Sutskever, and Geoffrey E Hinton. Imagenet classification with deep convolutional neural networks. In F. Pereira, C.J. Burges, L. Bottou, and K.Q. Weinberger, editors, *Advances in Neural Information Processing Systems*, volume 25. Curran Associates, Inc., 2012. URL [https://proceedings.neurips.cc/paper\\_files/paper/2012/file/c399862d3b9d6b76c8436e924a68c45b-Paper.pdf](https://proceedings.neurips.cc/paper_files/paper/2012/file/c399862d3b9d6b76c8436e924a68c45b-Paper.pdf).
- [19] Bin Li, Yin Li, and Kevin W Eliceiri. Dual-stream multiple instance learning network for whole slide image classification with self-supervised contrastive learning. In *Proceedings of the IEEE/CVF conference on computer vision and pattern recognition*, pages 14318–14328, 2021.
- [20] Tsung-Yi Lin, Piotr Dollár, Ross Girshick, Kaiming He, Bharath Hariharan, and Serge Belongie. Feature pyramid networks for object detection. In *Proceedings of the IEEE conference on computer vision and pattern recognition*, pages 2117–2125, 2017.
- [21] Baoyuan Liu, Min Wang, Hassan Foroosh, Marshall Tappen, and Marianna Pinsky. Sparse convolutional neural networks. In *Proceedings of the IEEE conference on computer vision and pattern recognition*, pages 806–814, 2015.
- [22] Xuanqing Liu, Hsiang-Fu Yu, Inderjit Dhillon, and Cho-Jui Hsieh. Learning to encode position for transformer with continuous dynamical model. In *International conference on machine learning*, pages 6327–6335. PMLR, 2020.
- [23] Yinhan Liu, Myle Ott, Naman Goyal, Jingfei Du, Mandar Joshi, Danqi Chen, Omer Levy, Mike Lewis, Luke Zettlemoyer, and Veselin Stoyanov. Ro{bert}a: A robustly optimized {bert} pretraining approach, 2020. URL <https://openreview.net/forum?id=SyxS0T4tvS>.
- [24] Ze Liu, Yutong Lin, Yue Cao, Han Hu, Yixuan Wei, Zheng Zhang, Stephen Lin, and Baining Guo. Swin transformer: Hierarchical vision transformer using shifted windows. In *Proceedings of the IEEE/CVF international conference on computer vision*, pages 10012–10022, 2021.
- [25] Zhuang Liu, Hanzi Mao, Chao-Yuan Wu, Christoph Feichtenhofer, Trevor Darrell, and Saining Xie. A convnet for the 2020s. In *Proceedings of the IEEE/CVF conference on computer vision and pattern recognition*, pages 11976–11986, 2022.
- [26] David G Lowe. Distinctive image features from scale-invariant keypoints. *International journal of computer vision*, 60:91–110, 2004.
- [27] Jiasen Lu, Christopher Clark, Sangho Lee, Zichen Zhang, Savya Khosla, Ryan Marten, Derek Hoiem, and Aniruddha Kembhavi. Unified-io 2: Scaling autoregressive multimodal models with vision, language, audio, and action. *arXiv preprint arXiv:2312.17172*, 2023.
- [28] Ming Y Lu, Drew FK Williamson, Tiffany Y Chen, Richard J Chen, Matteo Barbieri, and Faisal Mahmood. Data-efficient and weakly supervised computational pathology on whole-slide images. *Nature Biomedical Engineering*, 5(6):555–570, 2021.
- [29] Ofir Press, Noah Smith, and Mike Lewis. Train short, test long: Attention with linear biases enables input length extrapolation. In *International Conference on Learning Representations*, 2022. URL <https://openreview.net/forum?id=R8sQPpGCv0>.

- [30] Zhuchen Shao, Hao Bian, Yang Chen, Yifeng Wang, Jian Zhang, Xiangyang Ji, et al. Transmil: Transformer based correlated multiple instance learning for whole slide image classification. *Advances in neural information processing systems*, 34:2136–2147, 2021.
- [31] Peter Shaw, Jakob Uszkoreit, and Ashish Vaswani. Self-attention with relative position representations. In *Proceedings of the 2018 Conference of the North American Chapter of the Association for Computational Linguistics: Human Language Technologies, Volume 2 (Short Papers)*, pages 464–468, New Orleans, Louisiana, 2018. Association for Computational Linguistics. doi: 10.18653/v1/N18-2074. URL <https://aclanthology.org/N18-2074>.
- [32] Jianlin Su, Murtadha Ahmed, Yu Lu, Shengfeng Pan, Wen Bo, and Yunfeng Liu. Roformer: Enhanced transformer with rotary position embedding. *Neurocomputing*, 568:127063, 2024.
- [33] Wenhao Tang, Sheng Huang, Xiaoxian Zhang, Fengtao Zhou, Yi Zhang, and Bo Liu. Multiple instance learning framework with masked hard instance mining for whole slide image classification. In *Proceedings of the IEEE/CVF International Conference on Computer Vision*, pages 4078–4087, 2023.
- [34] Ashish Vaswani, Noam Shazeer, Niki Parmar, Jakob Uszkoreit, Llion Jones, Aidan N Gomez, Łukasz Kaiser, and Illia Polosukhin. Attention is all you need. In I. Guyon, U. Von Luxburg, S. Bengio, H. Wallach, R. Fergus, S. Vishwanathan, and R. Garnett, editors, *Advances in Neural Information Processing Systems*, volume 30. Curran Associates, Inc., 2017. URL [https://proceedings.neurips.cc/paper\\_files/paper/2017/file/3f5ee243547dee91fbd053c1c4a845aa-Paper.pdf](https://proceedings.neurips.cc/paper_files/paper/2017/file/3f5ee243547dee91fbd053c1c4a845aa-Paper.pdf).
- [35] Jingdong Wang, Ke Sun, Tianheng Cheng, Borui Jiang, Chaorui Deng, Yang Zhao, Dong Liu, Yadong Mu, Mingkui Tan, Xinggang Wang, et al. Deep high-resolution representation learning for visual recognition. *IEEE transactions on pattern analysis and machine intelligence*, 43(10): 3349–3364, 2020.
- [36] Minjie Wang, Da Zheng, Zihao Ye, Quan Gan, Mufei Li, Xiang Song, Jinjing Zhou, Chao Ma, Lingfan Yu, Yu Gai, Tianjun Xiao, Tong He, George Karypis, Jinyang Li, and Zheng Zhang. Deep graph library: A graph-centric, highly-performant package for graph neural networks. *arXiv preprint arXiv:1909.01315*, 2019.
- [37] Wenhao Wang, Enze Xie, Xiang Li, Deng-Ping Fan, Kaitao Song, Ding Liang, Tong Lu, Ping Luo, and Ling Shao. Pyramid vision transformer: A versatile backbone for dense prediction without convolutions. In *Proceedings of the IEEE/CVF international conference on computer vision*, pages 568–578, 2021.
- [38] Yunyang Xiong, Zhanpeng Zeng, Rudrasis Chakraborty, Mingxing Tan, Glenn Fung, Yin Li, and Vikas Singh. Nyströmformer: A nyström-based algorithm for approximating self-attention. In *Proceedings of the AAAI Conference on Artificial Intelligence*, volume 35, pages 14138–14148, 2021.
- [39] Jianwei Yang, Chunyuan Li, Pengchuan Zhang, Xiyang Dai, Bin Xiao, Lu Yuan, and Jianfeng Gao. Focal attention for long-range interactions in vision transformers. In M. Ranzato, A. Beygelzimer, Y. Dauphin, P.S. Liang, and J. Wortman Vaughan, editors, *Advances in Neural Information Processing Systems*, volume 34, pages 30008–30022. Curran Associates, Inc., 2021. URL [https://proceedings.neurips.cc/paper\\_files/paper/2021/file/fc1a36821b02abbd2503fd949bfc9131-Paper.pdf](https://proceedings.neurips.cc/paper_files/paper/2021/file/fc1a36821b02abbd2503fd949bfc9131-Paper.pdf).
- [40] Manzil Zaheer, Guru Guruganesh, Kumar Avinava Dubey, Joshua Ainslie, Chris Alberti, Santiago Ontanon, Philip Pham, Anirudh Ravula, Qifan Wang, Li Yang, et al. Big bird: Transformers for longer sequences. *Advances in neural information processing systems*, 33: 17283–17297, 2020.
- [41] Hongrun Zhang, Yanda Meng, Yitian Zhao, Yihong Qiao, Xiaoyun Yang, Sarah E Coupland, and Yalin Zheng. Dtf-d-mil: Double-tier feature distillation multiple instance learning for histopathology whole slide image classification. In *Proceedings of the IEEE/CVF Conference on Computer Vision and Pattern Recognition*, pages 18802–18812, 2022.